Products from Reactions of $[Mn_2O_2(O_2CCH_3)(tpen)]^{2+}$ in Acidic and Neutral Aqueous Media:[1] $[Mn_2(\mu\text{-}O)_2(\mu\text{-}O_2CCH_3)(tpen)]^{3+}$ and $[\{Mn_3(\mu\text{-}O)_4(OH)(tpen)\}_2(\mu\text{-}tpen)]^{6+}$

Samudranil Pal[†] and William H. Armstrong*,[†]

Department of Chemistry, University of California, Berkeley, California 94720

Received May 28, 1992

The mixed-valence compound $[Mn_2(\mu\text{-}O)_2(\mu\text{-}O_2CCH_3)(tpen)](ClO_4)_2\cdot 3H_2O$ (**2**·$3H_2O$) reacts to form $[Mn_2(\mu\text{-}O)_2(\mu\text{-}O_2CCH_3)(tpen)](ClO_4)_3$ (**3**) is acidic aqueous solution and in contrast is converted to $[\{Mn_3(\mu\text{-}O)_4(OH)(tpen)\}_2(\mu\text{-}tpen)](ClO_4)_6\cdot 4H_2O$ (**4**·$4H_2O$) in distilled water (tpen is *N,N,N′,N′*-tetrakis(2-pyridylmethyl)-1,2-ethanediamine). Both reactions were carried out in the presence of a large excess of perchlorate counterion. Syntheses, structures, and selected properties of **3** and **4** are reported. Compound **3** crystallizes as **3**·CH_3CN from a solution of CH_3CN and $C_6H_5CH_3$ (2:1) in the space group $P\bar{1}$ with a = 14.733 (3) Å, b = 14.815 (2) Å, c = 18.157 (2) Å, α = 85.392 (11)°, β = 80.014 (15)°, γ = 75.572 (14)°, V = 3777.2 (1) Å^3, and Z = 4. Structural parameters for **3** are consistent with both manganese ions being in the 4+ oxidation state. The cyclic voltammogram of **3** in CH_3CN exhibits IV,IV/IV,III and IV,III/III,III reductions at +0.90 and –0.13 V, respectively, vs SSCE. Compound **4** crystallizes as **4**·$8CH_3CN$ from CH_3CN–$C_6H_5CH_3$ (1:1) in the space group $P\bar{1}$ with a = 15.298 (8) Å, b = 15.391 (4) Å, c = 15.382 (4) Å, α = 114.80 (2)°, β = 115.09 (3)°, γ = 93.98 (3)°, V = 2839.6 (6) Å^3, Z = 1. The cation in **4** resides on an inversion center. Bond distances and angles in **4** confirm that all Mn atoms are in the +4 oxidation state. The structure of **4** consists of two $\{Mn_3O_4\}^{4+}$ units linked by one tpen moiety. The $\{Mn_3O_4\}^{4+}$ cores in **4** are distorted in a manner that is reminiscent of $[Mn_3O_4(OH)(bpea)_3]^{3+}$ (*J. Am. Chem. Soc.* **1992**, *114*, 6398–6406). The cyclic voltammogram of **4** in CH_3CN displays two irreversible reduction responses at +0.10 and –0.27 V vs SSCE. The EPR spectrum of **4**·$4H_2O$ in frozen CH_3CN–$C_6H_5CH_3$ is consistent with an $S = {}^3/_2$ ground-state origin. Both **3** and **4**·$4H_2O$ were also characterized by infrared and electronic spectral measurements.

Introduction

The water oxidation catalytic site in photosystem II (PSII) consists of a polynuclear manganese oxo aggregate whose precise structure has not been established.[2] While it is generally thought that there are four manganese ions grouped together at this active site, the recent report of Pauly and Witt[3] may provide impetus for re-examination of this commonly held notion. The presence of oxo (O^{2-}) bridging ligands between manganese ions in PSII can be inferred from interpretation of the fine structure in the extended region of the X-ray absorption spectrum (EXAFS) which indicates at least two Mn···Mn contacts of 2.7 Å per four Mn atoms.[4] To date, the only structural unit shown to be consistent with that relatively short distance for higher oxidation state manganese (+3, +4) is the $\{Mn_2(\mu\text{-}O)_2\}$ core. Thus it is reasonable to consider this unit as a substructure of the biological aggregate.

We and others are attempting to further refine the structure of the water oxidation active site by preparing low molecular weight models whose spectral and magnetic properties can be compared to those of the enzyme.[5] For example, we recently reported a tetranuclear complex, $[(Mn_2O_2)_2(tphpn)_2]^{4+}$,[6] that has a parallel polarization EPR spectrum that resembles the corresponding spectrum of PSII at the Kok S_1 oxidation level.[7] With the intent of more closely reproducing the spectral and reactivity properties of the PSII center, we have been attempting to replace the alkoxide bridging ligands in $[(Mn_2O_2)_2(tphpn)_2]^{4+}$ with oxo or hydroxo groups, among others. One hypothetical approach to such a target molecule is illustrated in Scheme I (see structure B). In an earlier study[8] it was demonstrated that when the species in Scheme I with the $\{Mn_2O_2(O_2CCH_3)\}$ core structure is capped by the tridentate ligand *N,N*-bis(2-pyridylmethyl)-ethylamine (bpea), the reaction product obtained from aqueous solution is the trinuclear species $[Mn_3O_4(OH)(bpea)_3]^{3+}$ (**1**) rather than a dimer of dimers (structure B). In this report we examine the consequence of linking two amino–dipyridyl units together forming the dimer-spanning hexadentate ligand tpen.[9] Specifically, we wished to address the issue of whether the products from reaction of the $Mn^{III}Mn^{IV}$ species $[Mn_2O_2(O_2CCH_3)tpen]^{2+}$ (**2**)[9] in water would be altered relative to the bpea case by this rather large structural perturbation of the ligand environment.

[†] Current address: Department of Chemistry, Merkert Chemistry Center, Boston College, Chestnut Hill, MA 02167.

(1) In this paper, boldface Arabic numbers may refer to either the cation or the neutral salt. Abbreviations used: photosystem II, PSII; EXAFS, extended X-ray absorption fine structure; EPR, electron paramagnetic resonance; IR, infrared; tpen, *N,N,N′,N′*-tetrakis(2-pyridylmethyl)-1,2-ethanediamine; bpea, *N,N*-bis(2-pyridylmethyl)ethylamine; bipy, 2,2′-bipyridine; phen, 1,10-phenanthroline; Me_3tacn, 1,4,7-trimethyl-1,4,7-triazacyclononane; 5-NO_2-sadpen, bis(3-((2-hydroxy-5-nitrobenzyl)imino)propyl)methylamine; TEAP, tetraethylammonium perchlorate; SSCE, saturated sodium calomel electrode.

(2) (a) Brudvig, G. W.; Beck, W. F.; dePaula, J. C. *Annu. Rev. Biophys. Chem.* **1989**, *18*, 25–26. (b) Govindjee; Coleman, W. *Sci. Am.* **1990**, *262*, 50–58. (c) Debus, R. J. *Biochim. Biophys. Acta*, in press. (d) *Manganese Redox Enzymes*; Pecoraro, V. L., Ed.; VCH: New York, 1992. (e) Renger, G.; Wydrzynski, T. *Biol. Met.* **1991**, *4*, 73–80. (f) Babcock, G. T. In *New Comprehensive Biochemistry: Photosynthesis*; Amesz, J., Ed.; Elsevier: Amsterdam, 1987; pp 125–158.

(3) The number of manganese ions associated with the water oxidation enzyme may be greater than 4 according to: Pauly, S.; Witt, H. T. *Biochim. Biophys. Acta* **1992**, *1099*, 211–218.

(4) (a) Kirby, J. A.; Robertson, A. S.; Smith, J. P.; Thompson, A. C.; Cooper, S. R.; Klein, M. P. *J. Am. Chem. Soc.* **1981**, *103*, 5529–5537. (b) George, G. N.; Prince, R. C.; Cramer, S. P. *Science* **1989**, *243*, 789–791. (c) Penner-Hahn, J. E.; Fronco, R. M.; Pecoraro, V. L.; Yocum, C. F.; Betts, S. D.; Bowlby, N. R. *J. Am. Chem. Soc.* **1990**, *112*, 2549–2557. (d) Sauer, K.; Yachandra, V. K.; Britt, R. D.; Klein, M. P. In ref 2d, pp 141–175.

(5) (a) Armstrong, W. H. In ref 2d, pp 261–286. (b) Pecoraro, V. L. In ref 2d, pp 197–231. (c) Wieghardt, K. *Angew. Chem., Int. Ed. Engl.* **1989**, *28*, 1153–1172. (d) Pecoraro, V. L. *Photochem. Photobiol.* **1988**, *48*, 249–264. (e) Christou, G. *Acc. Chem. Res.* **1989**, *22*, 328–335. (f) Brudvig, G. W.; Crabtree, R. H. *Prog. Inorg. Chem.* **1989**, *37*, 99–142. (g) Thorp, H. H.; Brudvig, G. W.; *New J. Chem.* **1991**, *15*, 479–490.

(6) Chan, M. K.; Armstrong, W. H. *J. Am. Chem. Soc.* **1991**, *113*, 5055–5057.

(7) Dexheimer, S. L.; Klein, M. P. *J. Am. Chem. Soc.* **1992**, *114*, 2821–2826.

(8) Pal, S.; Chan, M. K.; Armstrong, W. H. *J. Am. Chem. Soc.* **1992**, *114*, 6398–6406.

(9) Pal, S.; Gohdes, J. W.; Wilisch, W. C. A.; Armstrong, W. H. *Inorg. Chem.* **1992**, *31*, 713–716.

0020-1669/92/1331-5417$03.00/0

Scheme I

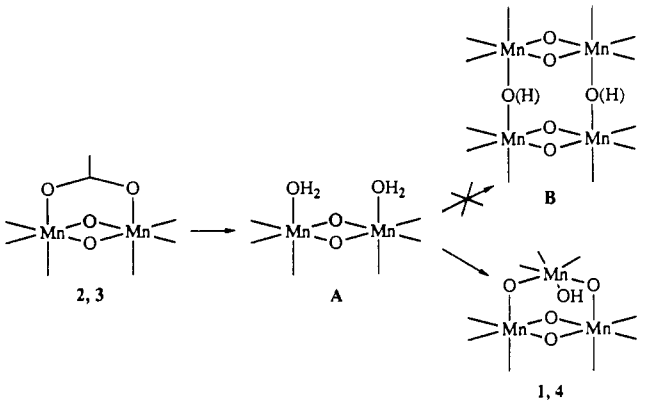

Also, it should be noted that removal of acetate from **2** and formation of structure A in Scheme I are desirable from the standpoint of testing a particular mechanism of water oxidation. It has been proposed that the crucial step in water oxidation, O–O bond formation, may take place between two terminally ligated O^{2-} or OH^- ligands across the face of an Mn_2O_2 unit in the PSII active site.[5] Another important motive for studying structural conversions[10] of polynuclear manganese complexes in aqueous media using model systems is that, by so doing, one may gain insight into the assembly of the PSII manganese center[11] and ideally assess the extent to which the polypeptide matrix influences the polynuclear manganese structure that forms.

Herein we show that $[Mn_2O_2(O_2CCH_3)(tpen)]^{2+}$ (**2**) reacts in aqueous solution to form two different products depending on the pH of the reaction medium. In acidic solution a portion of the dimanganese(III,IV) mixed-valence complex **2** remains intact and is converted to the IV,IV product $[Mn_2O_2(O_2CCH_3)(tpen)]^{3+}$ (**3**), while at higher pH decomposition to a species similar to **1** is observed: $[\{Mn_3O_4(OH)(tpen)\}_2(\mu\text{-tpen})]^{6+}$ (**4**). The synthesis of **4** from **3** is also demonstrated.

Experimental Section

Materials. The ligand tpen was prepared by following a reported procedure.[12] The starting material for the work described here, $[Mn_2O_2(O_2CCH_3)(tpen)](ClO_4)_2\cdot 3H_2O$ (**2**·$3H_2O$), was synthesized as described previously.[9] The supporting electrolyte TEAP and dry acetonitrile for electrochemistry were obtained by using reported methods.[9,13] All other solvents and chemicals were of analytical grade and used as received.

Physical Measurements. The X-band EPR spectrum of **4**·$4H_2O$ was recorded at 6 K using a Varian E-109 spectrometer equipped with an Air Products Model LTR liquid helium cryostat. All other measurements were performed as described earlier.[9]

Preparation of Compounds. $[Mn_2O_2(O_2CCH_3)(tpen)](ClO_4)_3$ (3). To a green acetonitrile solution (30 mL) of **2**·$3H_2O$ (300 mg, 0.34 mmol) was added 30 mL of an aqueous solution of 1 N $HClO_4$. The color of the solution changed to brown immediately. The mixture was allowed to stir in air at room temperature for 0.5 h. Concentration of the brown solution by slow evaporation provided a dark crystalline solid. This material was collected by filtration, washed with methanol, and dried under vacuum. The above procedure afforded 180 mg (54% yield) of **3**. Anal. Calcd for $Mn_2Cl_3O_{16}C_{28}H_{31}N_6$: Mn, 11.89; C, 36.40; H, 3.38; N, 9.10. Found: Mn, 11.7; C, 36.78; H, 3.55; N, 9.58. IR (cm^{-1}): 1610 (s), 1571 (w), 1545 (s), 1486 (s), 1437 (s), 1387 (s), 1340 (s), 1287 (m), 1252 (w), 1091 (br, vs), 1053 (m), 1032 (m), 930 (w), 769 (s), 681 (s), 637 (w), 625 (s). Symbols: br, broad; vs, very strong; s, strong; m, medium; w, weak.

$[Mn_6O_8(OH)_2(tpen)_3](ClO_4)_6\cdot 4H_2O$ (4·$4H_2O$). A green aqueous solution of **2**·$3H_2O$ (300 mg, 0.34 mmol) in 150 mL of distilled water was stirred in the air at room temperature for ~0.5 h. When the color of the solution became brownish, 2 g of solid $NaClO_4\cdot H_2O$ was added. The mixture was allowed to stir for another 10 h. A brown precipitate formed readily and was collected by filtration, washed with methanol, and dried under vacuum. This procedure provided a yield of 140 mg (50%, based on total Mn). Compound **4** can also be prepared from **3**. In this case, the procedure is the same as above except that **3** is dissolved in a CH_3CN–H_2O (1:9) mixture. The latter method affords improved yields of **4** (85%, based on total Mn). Anal. Calcd for $Mn_6Cl_6O_{38}C_{78}H_{94}N_{18}$: Mn, 13.54; C, 38.49; H, 3.89; N, 10.36. Found: Mn, 13.4; C, 38.39; H, 3.70; N, 10.26. IR (cm^{-1}): 3411 (br, s), 1610 (s), 1571 (w), 1481 (s), 1437 (s), 1287 (m), 1249 (w), 1091 (br, vs), 1053 (m), 1029 (m), 930 (w), 769 (s), 669 (s), 637 (w), 625 (s).

Table I. Crystallographic Data for $[Mn_2O_2(O_2CCH_3)(tpen)](ClO_4)_3\cdot CH_3CN$ (**3**·CH_3CN) and $[Mn_6O_8(OH)_2(tpen)_3](ClO_4)_6\cdot 8CH_3CN$ (**4**·$8CH_3CN$)

	3·CH_3CN	4·$8CH_3CN$
chem formula	$Mn_2Cl_3O_{16}N_7C_{30}H_{34}$	$Mn_6Cl_6O_{34}N_{26}C_{94}H_{110}$
fw	964.88	2690.42
temp, K	175	188
space group	$P\bar{1}$	$P\bar{1}$
a, Å	14.733 (3)	15.298 (8)
b, Å	14.815 (2)	15.391 (4)
c, Å	18.157 (2)	15.382 (4)
α, deg	85.392 (11)	114.80 (2)
β, deg	80.014 (15)	115.09 (3)
γ, deg	75.572 (14)	93.98 (3)
V, Å^3	3777.2 (14)	2839.6 (56)
Z	4	1
d_{calcd}, g cm^{-3}	1.697	1.577
μ, cm^{-1}	9.346	8.52
λ, Å	0.710 73	0.710 73
R,[a] %	3.83	6.67
R_w,[b] %	4.75	7.35

[a] $R = (\sum||F_o| - |F_c||)/\sum|F_o|$. [b] $R_w = \{[\sum w(|F_o| - |F_c|)^2]/\sum wF_o^2\}^{1/2}$; $w = 4F_o^2/[\sigma(I)^2 + (pF_o^2)^2]$, where $p = 0.03$.

X-ray Crystallography. Data collections for **3** and **4** were carried out with an Enraf-Nonius CAD4 diffractometer. In both cases, crystals were taken from the mother liquor and immediately coated with oil (Paratone N, Exxon Chemical Co.), mounted on a glass fiber, and quickly transferred to the nitrogen cold stream of the diffractometer. As the crystals of **4** are apparently extremely solvent loss sensitive, the oil was cooled to 273 K before being used to coat them. Unit cell dimensions were determined by the least-squares fit of 24 reflections (including Friedel pairs) having 2θ values within 22–24° (**3**) and 23–26° (**4**). Intensities of three reflections were measured after every 1 h to monitor the crystal stability. No decay was observed in the 59.8 h (**3**) and 62.5 h (**4**) of exposure to X-radiation. The ψ scans[14] of three reflections with θ values in the ranges 5–14° (**3**) and 6–12° (**4**) and χ in the ranges 83–87° (**3**) and 82–88° (**4**) were used for the empirical absorption corrections. The structures were solved by direct methods[15] and refined by full-matrix least-squares and Fourier techniques on a Digital Equipment MicroVAX computer using locally modified Enraf-Nonius SDP software.[16] Crystal parameters and refinement residuals are summarized in Table I. Specific individual features of the structure determinations for **3** and **4** are described below.

$[Mn_2O_2(O_2CCH_3)(tpen)](ClO_4)_3\cdot CH_3CN$ (3·CH_3CN). Single crystals were grown by slow evaporation of an acetonitrile–toluene (2:1) solution of **3**. Unit cell parameters indicated that the CH_3CN solvate crystallizes in the triclinic system. The structure was solved in the space group $P\bar{1}$. The asymmetric unit contains two molecules of **3** as well as two CH_3CN molecules. Among the six independent perchlorate ions, two are

(10) (a) Sarneski, J. E.; Thorp, H. H.; Brudvig, G. W.; Crabtree, R. H.; Schulte, G. K. *J. Am. Chem. Soc.* **1990**, *112*, 7255–7260. (b) Wang, S.; Folting, K.; Streib, W. E.; Schmitt, E. A.; McCusker, J. K.; Hendrickson, D. N.; Christou, G. *Angew. Chem., Int. Ed. Engl.* **1991**, *30*, 305–306.
(11) (a) Miller, A.-F.; Brudvig, G. W. *Biochemistry* **1990**, *29*, 1385–1392. (b) Tamura, N.; Chaniae, G. M. In *Progress in Photosynthesis Research*; Biggins, J., Ed.; Martinus Nijhoff: Dordrecht, The Netherlands, 1989; Vol. 1, pp 621–624.
(12) Mandel, J. B.; Maricondi, C.; Douglas, B. E. *Inorg. Chem.* **1988**, *27*, 2990–2996.
(13) Sawyer, D. T.; Roberts, J. L. *Experimental Electrochemistry for Chemists*; Wiley: New York, 1974, p 212.
(14) North, A. C. T.; Philips, D. C.; Mathews, F. S. *Acta Crystallogr., Sect. A* **1968**, *24*, 351–359.
(15) G. M. Sheldrick, SHELXS-86, a program for X-ray structure determination.
(16) Frenz, B. A. *Structure Determination Package*; Texas A&M University and Enraf-Nonius: College Station, TX, and Delft, The Netherlands, 1985 (as revised by Dr. F. J. Hollander).

Table II. Positional Parameters and Isotropic Equivalent Thermal Parameters[a] for the Two Cations of $[Mn_2O_2(O_2CCH_3)(tpen)](ClO_4)_3 \cdot CH_3CN$ in the Asymmetric Unit

atom	x	y	z	B, Å²	atom	x	y	z	B, Å²
Mn1	0.17494 (1)	0.28271 (1)	0.91960 (1)	1.70 (1)	C17	0.3679 (3)	0.4213 (3)	1.1486 (2)	2.5 (1)
Mn2	0.32646 (1)	0.32082 (1)	0.95003 (1)	1.61 (1)	C18	0.3844 (3)	0.5088 (3)	1.1305 (2)	2.8 (1)
Mn3	0.19583 (1)	0.77881 (1)	0.39733 (1)	1.50 (1)	C19	0.3860 (3)	0.5443 (3)	1.0577 (2)	2.4 (1)
Mn4	0.34484 (1)	0.82060 (1)	0.42915 (1)	1.51 (1)	C20	0.3730 (3)	0.4902 (3)	1.0041 (2)	2.1 (1)
O1	0.2041 (2)	0.3420 (2)	0.9918 (1)	1.77 (6)	C21	0.4699 (3)	0.1954 (3)	1.0247 (2)	2.3 (1)
O2	0.3010 (2)	0.2386 (2)	0.8937 (1)	1.77 (6)	C22	0.5183 (3)	0.2190 (3)	0.9491 (2)	1.84 (9)
O3	0.1718 (2)	0.3893 (2)	0.8495 (2)	2.02 (6)	C23	0.6130 (3)	0.1814 (3)	0.9246 (2)	2.6 (1)
O4	0.3026 (2)	0.4228 (2)	0.8759 (1)	1.91 (6)	C24	0.6533 (3)	0.2086 (3)	0.8546 (3)	2.9 (1)
O5	0.2207 (2)	0.8462 (2)	0.4666 (1)	1.71 (6)	C25	0.5982 (3)	0.2716 (3)	0.8107 (2)	2.4 (1)
O6	0.3220 (2)	0.7329 (2)	0.3769 (1)	1.64 (6)	C26	0.5048 (3)	0.3065 (3)	0.8377 (2)	2.09 (9)
O7	0.1962 (2)	0.8799 (2)	0.3219 (1)	1.82 (6)	C27	0.2326 (3)	0.4389 (3)	0.8404 (2)	1.86 (9)
O8	0.3259 (2)	0.9155 (2)	0.3491 (1)	1.91 (6)	C28	0.2198 (3)	0.5196 (3)	0.7865 (2)	2.8 (1)
N1	0.0354 (2)	0.3258 (2)	0.9589 (2)	2.08 (8)	C29	0.0038 (3)	0.9146 (3)	0.4205 (2)	2.3 (1)
N2	0.1484 (2)	0.2049 (2)	0.8426 (2)	1.89 (8)	C30	−0.0866 (3)	0.9463 (3)	0.4571 (3)	3.0 (1)
N3	0.1655 (2)	0.1661 (2)	0.9848 (2)	1.92 (8)	C31	−0.1255 (3)	0.8876 (4)	0.5088 (3)	3.5 (1)
N4	0.3632 (2)	0.2265 (2)	1.0341 (2)	1.79 (8)	C32	−0.0737 (3)	0.7977 (3)	0.5217 (3)	2.9 (1)
N5	0.3555 (2)	0.4055 (2)	1.0216 (2)	1.77 (7)	C33	0.0178 (3)	0.7698 (3)	0.4836 (2)	1.97 (9)
N6	0.4652 (2)	0.2816 (2)	0.9065 (2)	1.70 (7)	C34	0.0774 (3)	0.6734 (3)	0.4920 (2)	2.2 (1)
N7	0.0557 (2)	0.8275 (2)	0.4338 (2)	1.79 (7)	C35	0.1415 (3)	0.7181 (3)	0.2592 (2)	2.1 (1)
N8	0.1713 (2)	0.6929 (2)	0.3252 (2)	1.74 (7)	C36	0.1345 (3)	0.6520 (3)	0.2124 (2)	2.4 (1)
N9	0.1821 (2)	0.6677 (2)	0.4677 (2)	1.70 (7)	C37	0.1571 (3)	0.5594 (3)	0.2345 (2)	2.4 (1)
N10	0.3745 (2)	0.7355 (2)	0.5197 (2)	1.72 (7)	C38	0.1874 (3)	0.5328 (3)	0.3023 (2)	2.2 (1)
N11	0.4853 (2)	0.7768 (2)	0.3922 (2)	1.57 (7)	C39	0.1936 (3)	0.6013 (3)	0.3472 (2)	1.81 (9)
N12	0.3662 (2)	0.9151 (2)	0.4958 (2)	1.75 (7)	C40	0.2252 (3)	0.5823 (3)	0.4219 (2)	1.92 (9)
C1	−0.0201 (3)	0.4116 (3)	0.9462 (2)	2.5 (1)	C41	0.2274 (3)	0.6622 (3)	0.5371 (2)	1.94 (9)
C2	−0.1122 (3)	0.4370 (3)	0.9810 (3)	3.1 (1)	C42	0.3340 (3)	0.6504 (3)	0.5288 (2)	1.89 (9)
C3	−0.1488 (3)	0.3751 (3)	1.0314 (3)	3.5 (1)	C43	0.4816 (3)	0.7028 (3)	0.5155 (2)	2.2 (1)
C4	−0.0922 (3)	0.2884 (3)	1.0455 (3)	3.0 (1)	C44	0.5349 (3)	0.7188 (3)	0.4401 (2)	1.77 (9)
C5	−0.0004 (3)	0.2655 (3)	1.0075 (2)	2.3 (1)	C45	0.6302 (3)	0.6794 (3)	0.4206 (2)	2.5 (1)
C6	0.0623 (3)	0.1705 (3)	1.0145 (2)	2.5 (1)	C46	0.6755 (3)	0.6993 (3)	0.3499 (3)	2.7 (1)
C7	0.1184 (3)	0.2365 (3)	0.7771 (2)	2.2 (1)	C47	0.6246 (3)	0.7573 (3)	0.3004 (2)	2.2 (1)
C8	0.1107 (3)	0.1761 (3)	0.7265 (2)	2.7 (1)	C48	0.5298 (3)	0.7949 (3)	0.3230 (2)	1.93 (9)
C9	0.1307 (3)	0.0814 (3)	0.7446 (2)	2.9 (1)	C49	0.3348 (3)	0.7952 (3)	0.5867 (2)	2.2 (1)
C10	0.1598 (3)	0.0493 (3)	0.8118 (2)	2.6 (1)	C50	0.3556 (3)	0.8894 (3)	0.5693 (2)	2.03 (9)
C11	0.1690 (3)	0.1122 (3)	0.8605 (2)	2.04 (9)	C51	0.3574 (3)	0.9488 (3)	0.6233 (2)	2.8 (1)
C12	0.2044 (3)	0.0864 (3)	0.9333 (2)	2.2 (1)	C52	0.3691 (3)	1.0375 (3)	0.6008 (3)	3.2 (1)
C13	0.2172 (3)	0.1522 (3)	1.0518 (2)	2.2 (1)	C53	0.3792 (3)	1.0638 (3)	0.5265 (3)	2.7 (1)
C14	0.3242 (3)	0.1408 (3)	1.0385 (2)	2.1 (1)	C54	0.3783 (3)	1.0011 (3)	0.4748 (2)	2.2 (1)
C15	0.3282 (3)	0.2790 (3)	1.1054 (2)	1.92 (9)	C55	0.2562 (3)	0.9298 (3)	0.3131 (2)	1.85 (9)
C16	0.3521 (3)	0.3713 (3)	1.0936 (2)	1.86 (9)	C56	0.2435 (3)	1.0114 (3)	0.2593 (3)	2.8 (1)

[a] The thermal parameter given for anisotropically refined atoms is the isotropic equivalent thermal parameter defined as $(4/3)[a^2\beta(1,1) + b^2\beta(2,2) + c^2\beta(3,3) + ab(\cos\gamma)\beta(1,2) + ac(\cos\beta)\beta(1,3) + bc(\cos\alpha)\beta(2,3)]$ where a, b, and c, are real cell parameters and $\beta(i,j)$ are anisotropic β's.

disordered. The first one contains a pseudo-3-fold axis which passes through the Cl atom and a single fully occupied O atom. The other three O atoms are located in six positions around this 3-fold axis. In the second disordered perchlorate ion, the Cl atom is found in two positions. Two of the four O atoms are fully occupied and the other two are distributed among four sites. All non-hydrogen atoms except the O atoms having partial occupancies were refined using anisotropic thermal parameters. Hydrogen atoms were located on a difference Fourier map and included in the structure factor calculation at idealized positions, but neither their positions nor their thermal parameters were refined. Positional and isotropic equivalent thermal parameters for **3** are provided in Table II.

$[Mn_6O_8(OH)_2(tpen)_3](ClO_4)_6 \cdot 8CH_3CN$ ($4 \cdot 8CH_3CN$). Single crystals were obtained by slow evaporation of an acetonitrile–toluene (1:1) solution of $4 \cdot 4H_2O$. The structure was solved in the space group $P\bar{1}$. The cation resides on a crystallographic inversion center. Thus the asymmetric unit contains half of the hexanuclear cation, three perchlorate anions, and four acetonitrile molecules. All three of the three perchlorate ions are disordered. Two of them display similar disorder behaviors; a pseudo-3-fold axis passes through the Cl atom and a single fully occupied O atom. The other three O atoms are found in six positions around the 3-fold axis. In the third ClO_4^-, all four of the O atoms are disordered. They were located in a total of eight different sites. All non-hydrogen atoms with full occupancies were refined using anisotropic thermal parameters. Hydrogen atoms including that of the hydroxo group were located on a difference map and included in the structure factor calculation, but not refined. With the exception of the hydroxo group hydrogen atom, all hydrogen atoms were placed at idealized positions. Positional and isotropic equivalent thermal parameters for **4** are supplied in Table III.

Results and Discussion

Synthesis. Formation of **3** from **2** by treatment with acid is most likely the consequence of a disproportionation reaction. Disproportionation of dimanganese(III,IV) complexes under acidic conditions has been postulated previously.[10a,17] The first step in this process would probably involve protonation of a bridging oxo group. This protonation would make the III,IV complex a much stronger oxidant,[18] permitting it to oxidize an unprotonated III,IV species to the IV,IV level while the protonated species would be initially reduced to the III,III level. Since the filtrate of our reaction mixture was not very intensely colored, it would appear that the majority of the unisolated manganese is ultimately reduced to the +2 oxidation level. In contrast, manganese(III) and -(IV) complexes generally are intensely colored. A balanced equation that provides rationale for the behavior of **2** in acidic solution is given in eq 1. This equation

$$4Mn^{III}Mn^{IV}(O)_2 + 4H^+ \rightarrow 2Mn^{II}(H_2O) + 3Mn^{IV}{}_2(O)_2 \quad (1)$$

predicts a maximum yield of 75%, whereas we observe a 54% yield. It is interesting to note that **2** may be significantly more stable in acidic solution than is $[Mn^{III}Mn^{IV}O_2(bipy)_4]^{3+}$ and presumably $[Mn^{IV}{}_2O_2(bipy)_4]^{4+}$ as well. Sarneski et al. showed

(17) Cooper, S. R.; Calvin, M. *J. Am. Chem. Soc.* **1977**, *99*, 6623–6630.
(18) Thorp, H. H.; Sarneski, J. E.; Brudvig, G. W.; Crabtree, R. H. *J. Am. Chem. Soc.* **1989**, *111*, 9249–9250.

Table III. Positional Parameters and Isotropic Equivalent Thermal Parameters[a] for the Asymmetric Unit of $[Mn_6O_8(OH)_2(tpen)_3]^{6+}$

atom	x	y	z	B, Å²
Mn1	0.34382 (8)	0.60318 (8)	0.76037 (8)	1.69 (3)
Mn2	0.32130 (8)	0.74346 (8)	0.70526 (8)	1.79 (3)
Mn3	0.17384 (8)	0.70018 (8)	0.78964 (8)	1.61 (3)
O1	0.3967 (3)	0.7393 (3)	0.8311 (3)	1.8 (1)
O2	0.2986 (3)	0.6094 (4)	0.6338 (3)	1.8 (1)
O3	0.2313 (3)	0.5992 (3)	0.7710 (3)	1.7 (1)
O4	0.2048 (4)	0.7402 (4)	0.7091 (3)	1.9 (1)
O5	0.2784 (4)	0.7960 (4)	0.9253 (4)	2.3 (1)
N1	0.3041 (4)	0.4480 (4)	0.6767 (4)	1.9 (2)
N2	0.4231 (5)	0.6085 (4)	0.9114 (4)	2.1 (2)
N3	0.4752 (4)	0.5770 (4)	0.7535 (4)	2.2 (2)
N4	0.4535 (4)	0.7742 (5)	0.6956 (4)	2.3 (2)
N5	0.3684 (5)	0.8975 (5)	0.7925 (4)	2.3 (2)
N6	0.2584 (4)	0.7603 (4)	0.5685 (4)	2.1 (2)
N7	0.0325 (4)	0.5952 (4)	0.6480 (4)	1.4 (2)
N8	0.1113 (4)	0.6542 (5)	0.8647 (4)	2.1 (2)
N9	0.0810 (4)	0.7924 (4)	0.8004 (4)	2.0 (2)
C1	0.2296 (5)	0.3873 (5)	0.6672 (5)	1.9 (2)
C2	0.2023 (6)	0.2852 (6)	0.6017 (6)	2.6 (2)
C3	0.2516 (7)	0.2452 (6)	0.5430 (6)	3.2 (3)
C4	0.3281 (6)	0.3082 (6)	0.5557 (6)	2.7 (2)
C5	0.3550 (6)	0.4099 (6)	0.6233 (5)	2.3 (2)
C6	0.4386 (6)	0.4878 (6)	0.6441 (6)	2.6 (2)
C7	0.3946 (6)	0.6392 (6)	0.9872 (5)	2.2 (2)
C8	0.4604 (6)	0.6646 (6)	1.0953 (6)	3.1 (2)
C9	0.5561 (7)	0.6578 (7)	1.1236 (6)	4.0 (3)
C10	0.5853 (6)	0.6248 (6)	1.0448 (7)	3.5 (3)
C11	0.5162 (6)	0.5992 (5)	0.9374 (5)	2.2 (2)
C12	0.5354 (6)	0.5534 (6)	0.8432 (6)	3.0 (2)
C13	0.5444 (6)	0.6629 (6)	0.7703 (6)	2.8 (2)
C14	0.5085 (6)	0.6956 (6)	0.6833 (6)	3.0 (2)
C15	0.5237 (6)	0.8707 (6)	0.7996 (6)	2.7 (2)
C16	0.4653 (6)	0.9423 (6)	0.8256 (6)	2.7 (2)
C17	0.5037 (6)	1.0433 (6)	0.8801 (6)	3.0 (3)
C18	0.4441 (7)	1.1023 (6)	0.9065 (6)	3.8 (3)
C19	0.3480 (7)	1.0583 (6)	0.8745 (6)	3.4 (3)
C20	0.3113 (6)	0.9571 (6)	0.8173 (6)	2.8 (2)
C21	0.4261 (7)	0.7875 (7)	0.5959 (6)	3.7 (3)
C22	0.3197 (6)	0.7823 (6)	0.5362 (6)	2.3 (2)
C23	0.2864 (7)	0.8007 (7)	0.4478 (6)	4.1 (3)
C24	0.1855 (8)	0.7941 (8)	0.3926 (6)	4.9 (3)
C25	0.1203 (7)	0.7675 (7)	0.4238 (6)	4.1 (3)
C26	0.1603 (6)	0.7535 (6)	0.5142 (6)	2.7 (2)
C27	−0.0013 (5)	0.5248 (6)	0.6783 (5)	2.1 (2)
C28	0.0272 (5)	0.5760 (6)	0.7981 (5)	2.2 (2)
C29	−0.0247 (6)	0.5429 (6)	0.8363 (6)	3.0 (2)
C30	0.0076 (6)	0.5930 (7)	0.9482 (6)	3.8 (3)
C31	0.0899 (7)	0.6732 (7)	1.0155 (6)	3.7 (3)
C32	0.1423 (6)	0.7040 (7)	0.9739 (6)	3.2 (3)
C33	−0.0394 (5)	0.6522 (6)	0.6213 (5)	2.0 (2)
C34	−0.0168 (5)	0.7484 (6)	0.7208 (5)	2.3 (2)
C35	−0.0881 (6)	0.7969 (6)	0.7285 (6)	2.8 (2)
C36	−0.0602 (6)	0.8901 (6)	0.8173 (6)	3.2 (3)
C37	0.0399 (6)	0.9327 (6)	0.8969 (6)	3.4 (3)
C38	0.1090 (6)	0.8817 (6)	0.8874 (6)	2.8 (3)
C39	0.0470 (5)	0.5380 (5)	0.5514 (5)	1.6 (2)

[a] The thermal parameter given for anisotropically refined atoms is the isotropic equivalent thermal parameter defined as $(4/3)[a^2\beta(1,1) + b^2\beta(2,2) + c^2\beta(3,3) + ab(\cos\gamma)\beta(1,2) + ac(\cos\beta)\beta(1,3) + bc(\cos\alpha)\beta(2,3)]$ where a, b, and c are real cell parameters and $\beta(i,j)$ are anisotropic β's.

that at pH ~1.9 the III,IV bipyridyl complex is readily converted to a trinuclear species, $[Mn_3O_4(H_2O)_2(bipy)_4]^{4+}$ (**5**).[10a] There is no tendency for this reaction to take place for **2** in highly acidic media. The same can be said for a related species, $[Mn_2O_2(O_2CCH_3)(bpea)_2]^{3+}$ (**6**),[8] which was also prepared under acidic conditions. On the other hand, the relative stability of **2** and **6** in acid is comparable to that of $[Mn_2O_2(phen)_4]^{4+}$.[19] It should be noted that under the reaction conditions reported here, which include an excess of ClO_4^-, compound **3** is quite insoluble. It is possible that chemistry along the high-valent reaction channel

(19) Goodwin, H. A.; Sylva, R. N. *Aust. J. Chem.* **1967**, *20*, 629–637.

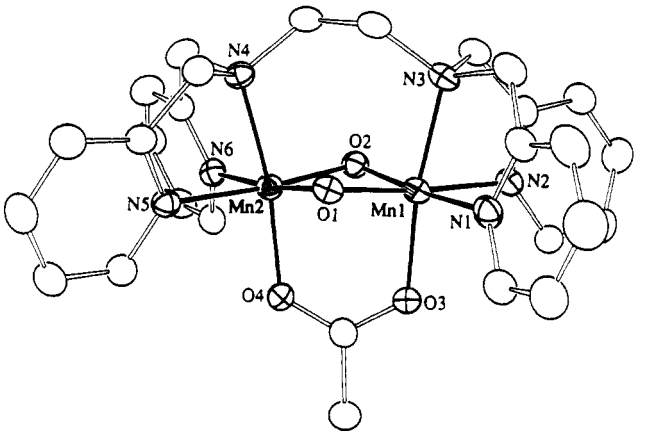

Figure 1. Crystal structure of $[Mn_2O_2(O_2CCH_3)(tpen)]^{3+}$ showing the 50% probability thermal ellipsoids. Hydrogen atoms are omitted, and carbon atoms are unlabeled for clarity.

subsequent to the initial disproportionation is blocked by precipitation of the IV,IV binuclear product.

When either compound **2** or **3** is dissolved in neutral water in the presence of excess ClO_4^-, reactions ensue that result in the precipitation of **4**, whose structure was shown to consist of a pair of $\{Mn_3O_4\}^{4+}$ aggregates linked together by a bridging tpen ligand (see below). As mentioned above, Sarneski et al. observed a similar reaction for the well-known mixed-valence III,IV complex $[Mn_2O_2(bipy)_4]^{3+}$.[10a] Recently, we reported a high-yielding synthesis of $[Mn_3O_4(OH)(bpea)_3]^{3+}$ (**1**) from the Mn(IV) dimer $[Mn_2O_2(O_2CCH_3)(bpea)_2]^{3+}$ (**6**).[8] Synthesis of **4** from the mixed-valence starting material **2** is relatively inefficient, providing a yield of 50%. As noted by Sarneski et al.,[10a] a disproportionation reaction in which 25% of the manganese ends up in the +2 oxidation state accounts, at least in part, for our lower yield when **2** is used as a starting material. On the other hand, when compound **3** is used as the starting material, no net redox chemistry is required; thus a higher yield of **4** is obtained (85%). Equation 2 illustrates one possible stoichiometry for this reaction. Thus,

$$3[Mn_2O_2(O_2CCH_3)(tpen)]^{3+} + 4H_2O \rightarrow [Mn_6O_8(OH)_2(tpen)_3]^{6+} + 3HO_2CCH_3 + 3H^+ \quad (2)$$

as we noted previously for the bpea supporting ligand,[8] one of every three dimers breaks up and is scavenged, resulting in the formation of the linked pair of trinuclear aggregates. Finally, it is important to emphasize that the synthesis of **4** is performed in the presence of excess counterion in order to facilitate its precipitation. When the reaction is run in the absence of added perchlorate, the principal product is an intractable brown solid. Analogous behavior was observed in our bpea system.[8]

Description of Structures. Compound **3** crystallizes in space group $P\bar{1}$ with two independent molecules in the asymmetric unit. The structure of one of the cations is illustrated in Figure 1. Selected bond distances and angles are listed in Table IV. Within experimental error, the distances and angles for each of the two cations are virtually identical. The average Mn–O distance (1.798 (3) Å) is comparable with the distances (1.75 (3)–1.819 (2) Å) reported for other dimanganese(IV) complexes.[8,20] While the Mn···Mn distance in **3** (2.591 (1) Å) is virtually identical to that in the one-electron-reduced analog **2**, it is significantly smaller than the distances (2.625 (2)–2.748 (2) Å) observed in bis(μ-oxo) species that lack bridging acetate groups. In **6**, the only other compound with the $\{Mn_2O_2(O_2CCH_3)\}^{3+}$ core, the Mn···Mn distance is 2.580 (1) Å.[8] As for all other $\{Mn_2O_2(O_2CCH_3)\}^{n+}$

Table IV. Selected Bond Distances (Å) and Angles (deg) for $[Mn_2O_2(O_2CCH_3)(tpen)](ClO_4)_3 \cdot CH_3CN$[a]

			Distances		
Mn1–O1	1.801 (3)	Mn2–O4	1.946 (3)	Mn3–N8	2.031 (3)
Mn1–O2	1.799 (3)	Mn2–N4	2.036 (3)	Mn3–N9	2.031 (3)
Mn1–O3	1.943 (3)	Mn2–N5	2.042 (3)	Mn4–O5	1.794 (3)
Mn1–N1	2.013 (4)	Mn2–N6	2.016 (3)	Mn4–O6	1.796 (3)
Mn1–N2	2.027 (3)	Mn3–O5	1.804 (3)	Mn4–O8	1.946 (3)
Mn1–N3	2.035 (3)	Mn3–O6	1.797 (3)	Mn4–N10	2.031 (3)
Mn2–O1	1.790 (3)	Mn3–O7	1.947 (3)	Mn4–N11	2.019 (3)
Mn2–O2	1.799 (3)	Mn3–N7	2.020 (3)	Mn4–N12	2.037 (3)
			Angles		
O1–Mn1–O2	86.0 (1)	O2–Mn2–N4	95.1 (1)	N7–Mn3–N8	92.3 (1)
O1–Mn1–O3	92.8 (1)	O2–Mn2–N5	174.9 (1)	N7–Mn3–N9	84.5 (1)
O1–Mn1–N1	91.0 (1)	O2–Mn2–N6	90.0 (1)	N8–Mn3–N9	80.0 (1)
O1–Mn1–N2	174.8 (1)	O4–Mn2–N4	170.9 (1)	O5–Mn4–O6	86.5 (1)
O1–Mn1–N3	94.4 (1)	O4–Mn2–N5	91.6 (1)	O5–Mn4–O8	92.5 (1)
O2–Mn1–O3	93.0 (1)	O4–Mn2–N6	92.5 (1)	O5–Mn4–N10	90.5 (1)
O2–Mn1–N1	174.2 (1)	N4–Mn2–N5	79.9 (1)	O5–Mn4–N11	173.4 (1)
O2–Mn1–N2	91.3 (1)	N4–Mn2–N6	84.4 (1)	O5–Mn4–N12	91.0 (1)
O2–Mn1–N3	91.1 (1)	N5–Mn2–N6	90.6 (1)	O6–Mn4–O8	93.3 (1)
O3–Mn1–N1	92.2 (1)	O5–Mn3–O6	86.1 (1)	O6–Mn4–N10	95.5 (1)
O3–Mn1–N2	91.8 (1)	O5–Mn3–O7	92.2 (1)	O6–Mn4–N11	90.2 (1)
O3–Mn1–N3	171.9 (1)	O5–Mn3–N7	88.9 (1)	O6–Mn4–N12	175.5 (1)
N1–Mn1–N2	91.3 (1)	O5–Mn3–N8	174.9 (1)	O8–Mn4–N10	170.8 (1)
N1–Mn1–N3	84.2 (1)	O5–Mn3–N9	95.3 (1)	O8–Mn4–N11	93.4 (1)
N2–Mn1–N3	81.1 (1)	O6–Mn3–O7	93.6 (1)	O8–Mn4–N12	90.4 (1)
O1–Mn2–O2	86.3 (1)	O6–Mn3–N7	172.9 (1)	N10–Mn4–N11	84.1 (1)
O1–Mn2–O4	93.1 (1)	O6–Mn3–N8	92.2 (1)	N10–Mn4–N12	80.8 (1)
O1–Mn2–N4	90.6 (1)	O6–Mn3–N9	90.9 (1)	N11–Mn4–N12	91.9 (1)
O1–Mn2–N5	92.6 (1)	O7–Mn3–N7	91.7 (1)	Mn1–O1–Mn2	92.4 (1)
O1–Mn2–N6	173.6 (1)	O7–Mn3–N8	92.7 (1)	Mn1–O2–Mn2	92.1 (1)
O2–Mn2–O4	93.4 (1)	O7–Mn3–N9	171.6 (1)	Mn3–O5–Mn4	92.1 (1)
Mn3–O6–Mn4	92.3 (1)				

[a] Numbers in parenthese are estimated standard deviations in the least significant digits.

(n = 2, 3) species,[8,9,21] the $\{Mn_2O_2\}$ core in **3** is not planar. The average dihedral angle between the planes containing Mn1, O1, O2 and Mn2, O1, O2 (Figure 1) for the two cations of **3** in the crystallographic asymmetric unit is 161.3 (3)°. Such a bending distortion and the resultant short Mn···Mn distance are clearly caused by the acetate bridge. The remaining bond lengths and angles for **3** (Table IV) are as expected for a dimanganese(IV) species.

As is evident from inspection of Figure 2b, hexanuclear compound **4** can be described as a dimer of trinuclear species. The cation has crystallographically imposed inversion symmetry in the solid state, and thus half of it is in the asymmetric unit (Figure 2a). The acetate bridge in **3** is replaced by an O–Mn–O bridging unit, and the two $\{Mn_3O_4\}^{4+}$ groups are bridged by one tpen moiety (Figure 2b). Structural parameters, shown in Table V, confirm that all manganese atoms in **4** are in the +4 oxidation state.[8,10a,22] While the $\{Mn_3O_4\}^{4+}$ units in **1**, **4**, **5**, and a related compound, $[Mn_3O_4Cl_2(bipy)_4]^{2+}$ (**7**),[22] are grossly similar, they fall into two different classes: (i) the lower symmetry (nearly C_s) cores, the dihedral angles between the planes containing Mn1, Mn2, O3, O4 and Mn3, O3, O4 being 26.6 and 28.8° for **1** and **4**, respectively; (ii) the more highly symmetric (nearly C_{2v}) cores, the defined dihedral angles for **5** and **7** being 0°. Perhaps one reason for the symmetry-lowering distortion in **1** and **4** is hydrogen bonding between the terminal OH group bound to Mn3 (Mn3–O5 = 1.830 Å in both **1** and **4**) and the bridging oxo group O1. The O1–O5 distances are 2.786 (5) Å for **1** and 2.743 (8) Å for **4**. Two other structurally characterized species with terminal Mn–OH bonds are known: $[Mn^{IV}_2O_2(OH)_2(tacn)_2]^{2+}$ (Mn–OH = 1.881 (5) Å)[20d] and $[Mn^{III}(5\text{-}NO_2\text{-}sadpen)(OH)]$ (Mn–OH = 1.827 (3) Å).[23] The average Mn–O distances in the basal $\{Mn_2(\mu\text{-}O)_2\}$ cores of **1** (1.813 (4) Å),[8] **4** (1.816 (5) Å), **5** (1.80 (1) Å),[10a] and **7** (1.819 (9) Å)[22] are very similar. However, one interesting feature observed in **1** is that the Mn–O1 distances (1.828 (4), 1.822 (4) Å) are longer than the Mn–O2 distances (1.797 (3), 1.807 (4) Å).[8] It was postulated that this asymmetry in the $\{Mn_2O_2\}$ core could be an effect of weakening the π-bonds to O1 as a consequence of the hydrogen bonding.[8] In contrast, there is no such difference in Mn–O1 and Mn–O2 distances in **4** (Table V). The average axial Mn–O distances (Mn1–O3 and Mn2–O4 in Figure 2a) in **1** (1.803 (4) Å) and **4** (1.801 (6) Å) are slightly smaller than those of **5** (1.84 (1) Å) and **7** (1.833 (10) Å). The Mn1···Mn2 (2.625 (2) Å) and Mn···Mn3 (average 3.192 (2) Å) distances in **4** are very similar to those of **1**, **5**, and **7**. As for **3**, the $\{Mn_2(\mu\text{-}O_2)\}$ core portion of **4** is not planar, with a dihedral angle of 159.9 (2)°. The corresponding dihedral angles for **1** (161.4°) **5** (163.6°), and **7** (163.8°) provide further evidence that the bridging O–Mn–O group in the trinuclear structures distorts the $\{Mn_2O_2\}$ rhomb to about the same extent as does the acetate ligand in complexes with $\{Mn_2O_2(O_2CCH_3)\}$ cores (see above). Finally, it should be noted that the $\{Mn_2O_2\}$ core in $[Mn_2O_2(O_2)(Me_3tacn)_2]^{2+}$ is significantly more puckered, with a dihedral angle of 138.2°.[20h]

(20) (a) Goodson, P. A.; Glerup, J.; Hodgson, D. J.; Michelsen, K.; Weihe, H. *Inorg. Chem.* **1991**, *30*, 4909–4914. (b) Goodson, P. A.; Glerup, J.; Hodgson, D. J.; Michelsen, K.; Pedersen, E. *Inorg. Chem.* **1990**, *29*, 503–508. (c) Oki, A. R.; Glerup, J.; Hodgson, D. J. *Inorg. Chem.* **1990**, *29*, 2435–2441. (d) Weighardt, K.; Bossek, U.; Nuber, B.; Weiss, J.; Bonvoisin, J.; Corbella, M.; Vitols, S. E.; Girerd, J.-J. *J. Am. Chem. Soc.* **1988**, *110*, 7398–7411. (e) Libby, E.; Webb, R. J.; Streib, W. E.; Folting, K.; Huffman, J. C.; Hendrickson, D. N.; Christou, G. *Inorg. Chem.* **1989**, *28*, 4037–4040. (f) Gohdes, J. W.; Armstrong, W. H. *Inorg. Chem.* **1992**, *31*, 368–373. (g) Larson, E.; Lah, M. S.; Li, X.; Bonadies, J. A.; Pecoraro, V. L. *Inorg. Chem.* **1992**, *31*, 373–378. (h) Bossek, U.; Weyhermuller, T.; Wieghardt, K.; Nuber, B.; Weiss, J. *J. Am. Chem. Soc.* **1990**, *112*, 6387–6388. (i) Stebler, M.; Ludi, A.; Burgi, H.-B. *Inorg. Chem.* **1986**, *25*, 4743–4750. (j) Gohdes, J. W. Ph.D. Dissertation, University of California, Berkeley, 1991.

(21) (a) Wieghardt, K.; Bossek, U.; Zsolnai, L.; Huttner, G.; Blondin, G.; Girerd, J.-J.; Babonneau, F. *J. Chem. Soc., Chem. Commun.* **1987**, 651–653. (b) Bashkin, J. S.; Schake, A. R.; Vincent, J. B.; Chang, H.-R.; Li, Q.; Huffman, J. C.; Christou, G.; Hendrickson, D. N. *J. Chem. Soc., Chem. Commun.* **1988**, 700–702.

(22) Auger, N.; Girerd, J.-J.; Corbella, M.; Gleizes, A.; Zimmermann, J.-L. *J. Am. Chem. Soc.* **1990**, *112*, 448–450.

(23) Eichhorn, D. M.; Armstrong, W. H. *J. Chem. Soc., Chem. Commun.* **1992**, 85–87.

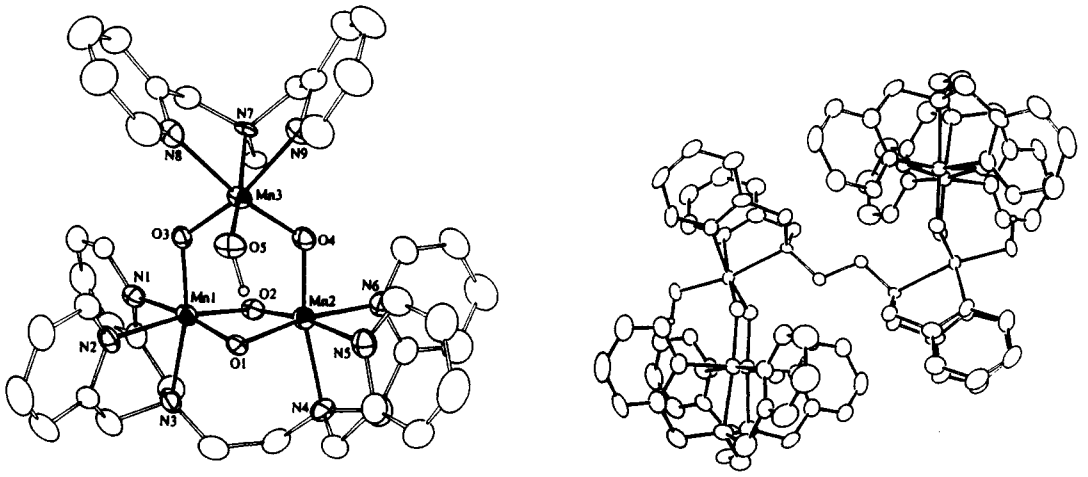

Figure 2. ORTEP plots of $[Mn_6O_8(OH)_2(tpen)_3]^{6+}$: (a) half of the cation in the asymmetric unit; (b) full view of the cation. All atoms are represented by their 50% probability thermal ellipsoids.

Table V. Selected Bond Distances (Å) and Angles (deg) for $[Mn_6O_8(OH)_2(tpen)_3](ClO_4)_6 \cdot 8CH_3CN$[a]

			Distances		
Mn1–O1	1.825 (5)	Mn2–O1	1.817 (5)	Mn3–O3	1.817 (5)
Mn1–O2	1.817 (6)	Mn2–O2	1.805 (5)	Mn3–O4	1.798 (7)
Mn1–O3	1.796 (6)	Mn2–O4	1.806 (6)	Mn3–O5	1.830 (3)
Mn1–N1	2.070 (6)	Mn2–N4	2.125 (8)	Mn3–N7	2.145 (4)
Mn1–N2	2.076 (7)	Mn2–N5	2.053 (6)	Mn3–N8	2.068 (8)
Mn1–N3	2.115 (7)	Mn2–N6	2.048 (7)	Mn3–N9	2.083 (7)
			Angles		
O1–Mn1–O2	85.3 (2)	O1–Mn2–O2	85.9 (2)	O3–Mn3–O4	96.8 (3)
O1–Mn1–O3	98.2 (2)	O1–Mn2–O4	98.2 (3)	O3–Mn3–O5	97.7 (2)
O1–Mn1–N1	170.7 (3)	O1–Mn2–N4	89.8 (3)	O3–Mn3–N7	89.5 (2)
O1–Mn1–N2	89.0 (2)	O1–Mn2–N5	90.7 (2)	O3–Mn3–N8	90.2 (3)
O1–Mn1–N3	93.2 (2)	O1–Mn2–N6	170.6 (3)	O3–Mn3–N9	167.7 (3)
O2–Mn1–O3	99.8 (2)	O2–Mn2–O4	96.9 (2)	O4–Mn3–O5	96.8 (2)
O2–Mn1–N1	92.9 (2)	O2–Mn2–N4	93.1 (3)	O4–Mn3–N7	92.2 (2)
O2–Mn1–N2	168.9 (3)	O2–Mn2–N5	171.8 (3)	O4–Mn3–N8	169.3 (2)
O2–Mn1–N3	89.3 (3)	O2–Mn2–N6	97.5 (2)	O4–Mn3–N9	91.2 (3)
O3–Mn1–N1	91.1 (3)	O4–Mn2–N4	167.6 (3)	O5–Mn3–N7	167.7 (3)
O3–Mn1–N2	90.5 (3)	O4–Mn2–N5	91.0 (3)	O5–Mn3–N8	90.3 (2)
O3–Mn1–N3	165.9 (3)	O4–Mn2–N6	90.2 (3)	O5–Mn3–N9	90.7 (2)
N1–Mn1–N2	91.2 (2)	N4–Mn2–N5	97.4 (3)	N7–Mn3–N8	79.7 (2)
N1–Mn1–N3	77.6 (3)	N4–Mn2–N6	81.3 (3)	N7–Mn3–N9	80.7 (2)
N2–Mn1–N3	81.4 (3)	N5–Mn2–N6	84.8 (2)	N8–Mn3–N9	80.7 (3)

[a] Numbers in parentheses are the estimated standard deviations in the least significant digits.

Redox Behavior. Cyclic voltammetry of **3** in acetonitrile at a Pt electrode reveals quasi-reversible ($E_{1/2}$ = +0.90 V, ΔE_p = 80 mV) and irreversible (E_{pc} = –0.13 V)[24] reduction responses. These are assigned to IV,IV/III,IV and III,IV/III,III reduction processes. As expected, the potentials for these two redox couples are identical with those observed for **2**.[9] Under the same conditions, two irreversible reduction responses at much lower potentials (E_{pc} = +0.10 and –0.27 V) are observed for **4**. In contrast, both **1** and **5** each display only a single reduction wave at $E_{1/2}$ = +0.04 V (ΔE_p = 80 mV) and E_{pc} = +0.36 V, respectively.

IR Spectra. As we pointed out for the corresponding bpea species,[8] infrared spectroscopy can be used very effectively to distinguish compounds **3** and **4**. Compound **3** shows the characteristic ν_{as} and ν_s stretches of the μ-acetate group at 1545 and 1387 cm^{-1}.[8,9,21] As expected, these peaks are absent in **4**. A sharp, intense peak at 681 cm^{-1} is observed for **3**. Absorptions in this region for compounds with an $\{Mn_2O_2\}$ core structure are typical[8,9,17,20,21] and assigned to a vibrational mode of the $\{Mn_2O_2\}$ unit. It is interesting to note that the III,IV analog (**2**) has a peak in virtually the same location. In the case of **4**, a relatively stronger and broader band is observed at 669 cm^{-1}. The comparable vibration for bpea analog **1** occurs at 672 cm^{-1}. The origin of this latter absorption is most likely a vibration involving the basal $\{Mn_2O_2\}$ portion of the trinuclear complex.

Electronic Spectra. The electronic absorption spectrum of **3** in acetonitrile (not shown) displays a shoulder at 630 nm and peaks at 590 nm (ϵ = 395 M^{-1} cm^{-1}) and 440 nm (ϵ = 1570 M^{-1} cm^{-1}). Bands in this spectral region have been observed for other IV,IV dioxo-bridged dimanganese complexes and assigned as oxo to metal $d\pi^*$ charge-transfer transitions.[20c] In contrast, related absorptions for dimanganese(III,IV) compounds have been assigned as d–d bands.[17] A band at 800 nm (ϵ = 50 M^{-1} cm^{-1}) and an intense shoulder at 320 nm are also observed for **3**. Low-energy absorptions in the region 800–900 nm have been reported[20j] for other dimanganese(IV) compounds; however the origin of these bands remains poorly understood. The spectrum of **4**·4H_2O in acetonitrile is quite distinct from that of **3** in terms of band shapes, with three shoulders at 420, 660, and 800 nm.

EPR Spectrum. Previously, we noted that there is a dramatic difference in the EPR spectrum of **1** at 6 K when compared to that of **5** or **7**, despite the fact that they all contain the $\{Mn_3O_4\}^{4+}$

(24) The potentials are referenced against the saturated sodium calomel electrode (SSCE). Symbols: E_{pa}, anodic peak potential; E_{pc}, cathodic peak potential; $E_{1/2} = (E_{pa} + E_{pc})/2$; $\Delta E_p = E_{pa} - E_{pc}$.

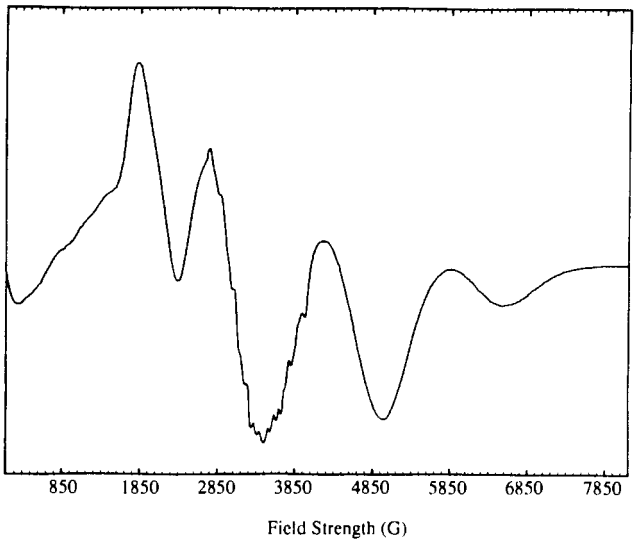

Figure 3. X-Band EPR spectrum of $4{\cdot}4H_2O$ in frozen (6 K) CH_3CN–$C_6H_5CH_3$ (1:1).

unit.[8] The spectrum of **1** exhibits features ($g_\perp = 3.6$, $g_\parallel = 1.92$) characteristic of a nearly axial $S = {}^3/_2$ system.[8] The X-band spectra of compounds **5** and **7** show signals centered at $g \sim 2$ with 35 resolved ^{55}Mn hyperfine lines.[10a,22] Variable-temperature magnetic susceptibility studies confirmed that the difference in the ground spin states, $S = {}^3/_2$ for **1**[8] and $S = {}^1/_2$ for **5**[10a] and **7**,[22] accounts for the different spectral behaviors. The X-band EPR spectrum of $4{\cdot}4H_2O$, shown in Figure 3, is significantly more complex than that of **1**, with several transitions in the range 800–7000 G. The fine structure in the region ~2900–3950 G apparent in Figure 3 is attributable to a small amount of an impurity of compound **2**. Despite the distinct difference in the appearance of the spectrum of **4** compared to that of **1**,[8] it is clear that the origin of the signal in Figure 3 is also an $S = {}^3/_2$ ground state.[25]

It is useful to consider certain features associated with mononuclear $S = {}^3/_2$ spin systems in order to rationalize the EPR spectrum of **4**. A d^3 ion having the $^4A_{2g}$ ground electronic state in a crystal field of ideal octahedral symmetry shows an isotropic $g = 2$ resonance.[26] Distortion and spin–orbit coupling splits the ground-state quartet into two Kramers doublets separated by $2(D^2 + E^2)^{1/2}$, where D and E are axial and rhombic zero-field-splitting parameters. The magnitudes of D, E, and the microwave quantum $h\nu$ (ca. 0.31 cm^{-1} at X-band) have been shown to determine the nature of the EPR spectrum for a d^3 system.[27] The same arguments may be applied to polynuclear $S = {}^3/_2$ systems. Two limiting conditions are (i) $2D \gg h\nu$, where strong $g = 4$ and weak $g = 2$ signals are observed, and (ii) $2D \ll h\nu$, where weak $g = 4$ and intense $g = 2$ signals are seen. The ideal octahedrally symmetric mononuclear case mentioned above falls into the second category. On the other hand, the EPR spectrum of the trinuclear bpea complex $[Mn_3O_4(OH)(bpea)_3]^{3+}$ (**1**) is clearly consistent with the limiting condition (i).[8] The D value for **4** appears to fall between these two extremes. Complex spectra, qualitatively similar to that for **4**, have been observed for other $S = {}^3/_2$ systems, including certain Cr(III) complexes.[27c]

Concluding Remarks. Our original goal of removing the acetate group from $[Mn_2O_2(O_2CCH_3)(tpen)]^{2+}$ (**2**) while keeping the oxo-bridged core intact was not fully realized. In acidic solution, a disproportionation reaction takes place that produces the Mn^{IV}_2 analog **3** as one product. In contrast, when **2** or **3** is dissolved in distilled water in the presence of excess perchlorate, conversion to the hexanuclear species $[Mn_6O_8(OH)_2(tpen)_3]^{6+}$ is observed. The hexanuclear complex consists of two weakly interacting trinuclear species of the type we recently identified for the tridentate bpea ligand,[8] which is essentially half of the hexadentate ligand studied here, tpen. Whereas the dimanganese(IV) species **3** is relatively stable in acidic solution, the related bipy-ligated complex is converted to a trinuclear species in acidic media.[10a] By continuing to study these types of core conversion processes, we hope to discover novel, fundamentally interesting manganese oxo compounds and to gain insight as to how the manganese-binding site in photosystem II influences the assembly of the polynuclear manganese aggregate that makes up the water oxidation catalyst.

Acknowledgment. Funding for this work was provided by Grant No. GM 382751 from the National Institute of General Medical Sciences. We thank Melissa Grush for assistance with the EPR spectral measurement.

Supplementary Material Available: Fully labeled ORTEP drawings (Figures S1 and S2), crystal data and data collection parameters (Table S1), atomic positional parameters (Tables S2 and S6), anisotropic thermal parameters (Tables S3 and S7), intramolecular bond distances (Tables S4 and S8), and intramolecular bond angles (Tables S5 and S9) for $3{\cdot}CH_3CN$ and $4{\cdot}8CH_3CN$ (21 pages). Ordering information is given on any current masthead page.

(25) Results of magnetic susceptibility measurements and EPR spectral simulations will be presented elsewhere.

(26) (a) Mowes, P. *Inorg. Chem.* **1966**, *5*, 5–8. (b) McGarvey, B. R. In *Transition Metal Chemistry*; Carlin, R. L., Ed.; Marcel Dekker: New York, 1966; Vol. 3, pp 163–167.

(27) (a) Singer, L. S. *J. Chem. Phys.* **1955**, *23*, 379–388. (b) Hempel, J. C.; Morgan, L. O.; Lewis, W. B. *Inorg. Chem.* **1970**, *9*, 2064–2072. (c) Pedersen, E.; Toftlund, H. *Inorg. Chem.* **1974**, *13*, 1603–1612.